Journal of Himalayan Earth Sciences 46(1) (2013) 19-30

# Petrology and geochemistry of gabbros from the Muslim Bagh Ophiolite: implications for their petrogenesis and tectonic setting

**Mohammad Ishaq Kakar[1], Khalid Mahmood[2], Mehrab Khan[3], Aimal Khan Kasi[1] and Razzaq Abdul Manan[1]**

[1]Centre of Excellence in Mineralogy, University of Balochistan, Quetta, Pakistan
[2]Department of Earth Sciences, University of Sargodha, Sargodha, Pakistan
[3]Department of Geology, University of Balochistan, Quetta, Pakistan

**Abstract**

The Muslim Bagh ophiolite has almost a complete ophiolite sequence with thick mantle section and comparatively less well-developed crustal section. The crustal part of the ophiolite occupiesan area of about 130 km$^2$, having both ultramafic cumulates; dunite, wherlite and pyroxenite and mafic cumulates or gabbros. The gabbros are olivine gabbro, pyroxene gabbro and hornblende gabbro. They are distinguished into cumulates and non-cumulates. Geochemical features indicate that they are tholeiitic and are formed in an arc-related tectonic setting. On NMORB normalized pattern of gabbros the HFS-elements (P, Zr, Sm, Ti, and Y) show a flat pattern parallel to NMORB. In contrast, the LIL-elements (Rb, Ba, Th, Sr) are relatively more enriched than NMORB. The enrichment of LIL-elements over the HFS-elements and the depletion of Nb relative to other HFS-elements suggest involvement of subduction component in the depleted mantle source, and suggest that they are formed in a supra-subduction zone tectonic setting.

*Keywords:* Muslim Bagh Ophiolite; Gabbros; Petrology; Geochemistry; Petrogenesis; Tectonic setting

## 1. Introduction

Gabbros are created by the injection of basaltic melt from the underlying rising mantle and are regarded as formed by slow crystallization in a magma chamber. They are an integral part of the crustal section in an ophiolite suite and may range at the base from layered gabbros to isotropic to foliated gabbros at the top. Some ophiolites have a well-developed gabbroic section e.g. Semail ophiolite Oman (e.g., Nicolas, 1989), and Bay of Island ophiolite, Newfoundland, Canada (e.g., Bedard, 1991). Unlike these ophiolites the Muslim Bagh ophiolite has a less developed gabbroic section and its crustal part and consists of cyclic succession of ultrmafic-mafic cumulates at the base which grades upward into foliated gabbros. The geological characteristics of crustal part from the Muslim Bagh ophiolite have been reported earlier by many workers (cf. Ahmed and Abbas, 1979; Mahmood et al., 1995; Mahmood and Khan, 1999; Siddiqui et al., 1996; Khan et al., 2007). However, no detailed study has been made of the geochemical characters of its gabbroic rocks. In this paper we are going to discuss the petrogenesis and tectonic setting of the gabbros from Muslim Bagh ophiolite using their field features, petrography and geochemistry.

## 2. The Muslim Bagh ophiolite

The Muslim Bagh ophiolite is part of the ophiolite belt; Waziristan–Muslim Bagh–Bela, which marks the NW and western boundary of the Indian plate with the Afghan block (Asrarullah et al. 1979; Siddiqui et al., 1996). The ophiolite comprises two main blocks called Jang Tor Ghar Massif (JTGM west) and Saplai Tor Ghar Massif (STGM east) (Bilgrami, 1964; Fig.1). The two blocks are structurally related and belong to the same ophiolite nappe. The JTGM is mainly composed of foliated peridotites (harzburgite and dunite) and covers an area of about 150 Km$^2$. The harzburgite consist of enstatite 25-30 %, olivine 5-10%, serpentine 55-60% and spinel 3-5%.The best preserved series of subophiolitic metamorphic rocks is located at the north-western side of the JTGM showing inverted metamorphic gradients. The metamorphic rock series comprised ofgarnet amphibolites facies grades downwards into amphibolites facies and greenshcist facies with calcite–marble inter layers.

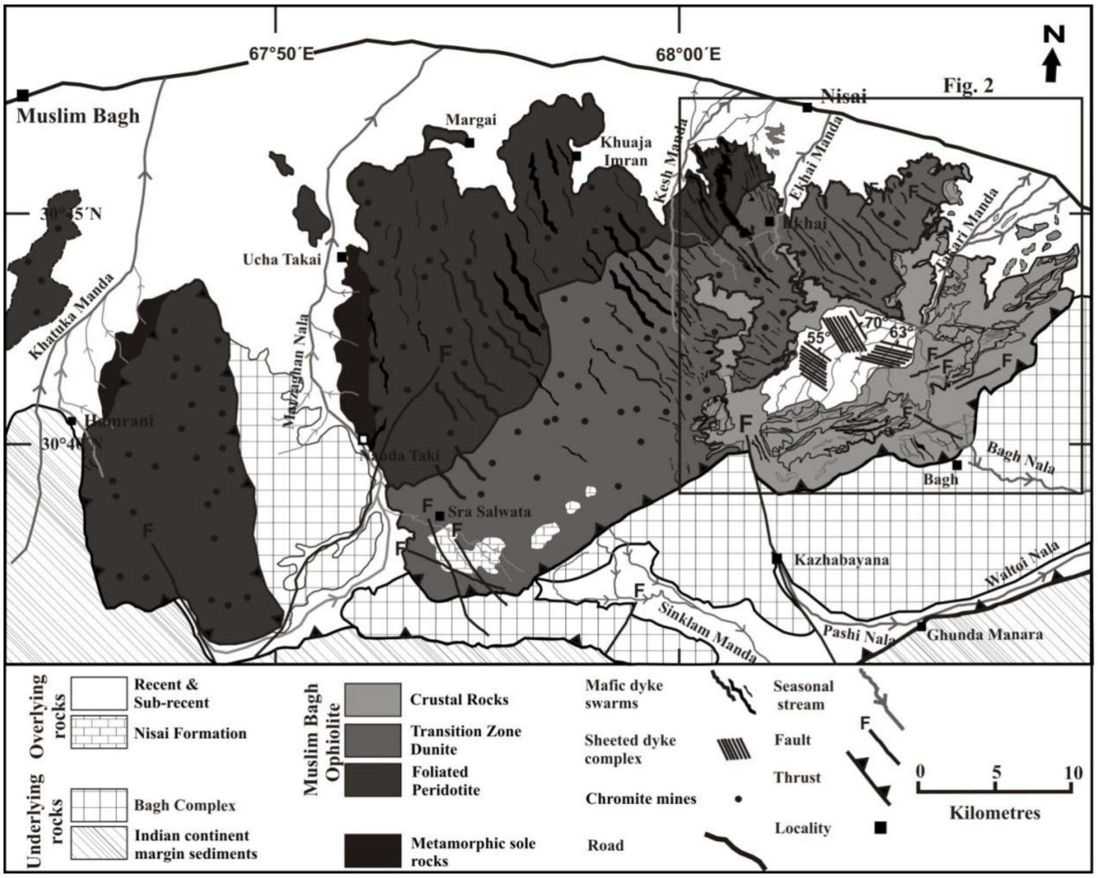


Fig. 1. Geological Map of the Muslim Bagh ophiolite, (modified after Van Vloten 1967; Siddiqui et al. 1996) and this study.

The STGM of the Muslim Bagh ophiolite shows a nearly complete ophiolitic sequence, as defined by the Penrose conference (1972), only the uppermost unit consisting of extrusive rocks and related sediments is missing (Fig.1). The sequence of the various rock units of STGM start at the base from the metamorphic sole rocks which is lithologically similar to that below the JTGM though less complete. The sole rocks are overlain by the foliated peridotites (harzburgite and dunite) of the mantle section which are usually serpentinized. The serpentinites are massive and vary in colour from light green to brownish green. Serpentinization is more pronounced in the areaof Crust Mantle Transition Zone. The duniteis the second most abundant rock type in the mantle section of STGM. There is a complete gradation from strongly depleted harzburgite to dunite in STGM near Nisai area (Fig. 1). Many outcrops of dunite contain large concentrations of chromite, which are being mined, locally in the areas. The structures in these mineable chromite bodies are concordant to host dunite.

One of the interesting features of the Muslim Bagh ophiolite is the presence of huge mafic dykes cross cutting the ophiolite at all structural levels. They are about 3-15 metres thick trending NW-SE (Fig.1-2). At places these dykes are broken and are strongly sheared along with country rocks forming boudinage bodies.

The crustal section of Muslim Bagh ophiolite is exposed in the eastern portion of the STGM (Fig. 1). It occupies an area of about 130 $km^2$ (Fig. 2). It comprises of cyclic successions of layered dunite, wehrlite, pyroxenite and both layered and foliated gabbro. The gabbroic section is followed by a less developed sheeted dyke complex. The sheeted dykes were originally dolerites but metamorphosed to amphibolite /greenschist. The complex is intruded at the base and in the middle part by plagiogranite and that has a consistent stratigraphic position with gabbroic rocks.

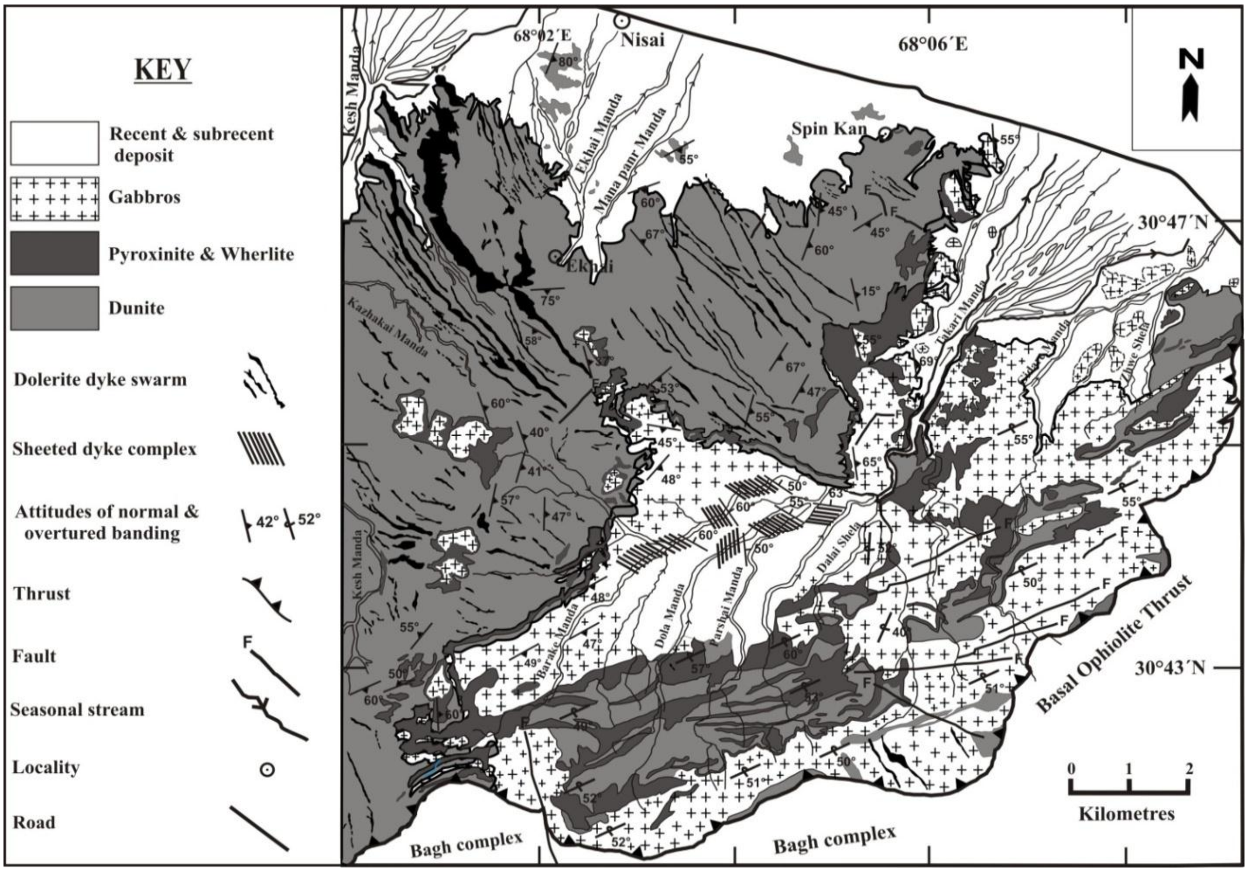


Fig. 2. Geological map of the crustal part of the Muslim Bagh ophiolite.

## 3. Gabbros

### *3.1. Petrology*

The mafic cumulate (gabbros) section is about 600 metres thick (Siddiqui et al., 1996). Besides crustal gabbros, some isolated gabbroic plutons cut the mantle rocks (Fig. 2). Field observations reveal that these gabbro plutons (isolated mini-magma chambers) appear to have been fed by many dykes. When the base of the gabbro pluton is approached, the dykes become less apparent and a transition zone develops between the top of dykes and the base of the gabbro (Khan et al., 2007). The mafic cumulate include olivine gabbro, norite, gabbro-norite, and hornblende gabbro.

Structurally, the gabbroic rocks can be divided into layered (Fig. 3a) and foliated gabbro. The layered gabbros are less well developed, the gradual layering was not observed, except in the south of the sheeted dyke complex (Fig. 3b). Most of the gabbros are plastically deformed and exhibit granular, porphyroclastic and mylonitic textures. The magmatic textures in the gabbros are generally absent and can only be observed at some localities. The syn-kinematic deformation occurred when the gabbros were still hot, probably in the vicinity of the ridge. The distribution of the syn-kinematic assemblage in the gabbros indicates that this deformation occurred at progressively decreasing temperature, as may be expected in an oceanic domain, where newly accreted lithosphere spreads away from a ridge axis (Nicolas, 1989; Mahmood et al., 1995; Mahmood and Khan, 1999). The gabbros feed a poorly developed sheeted dyke complex at the top with no extrusive cover.

Petrographically gabbroic rocks are melanocratic, holocrystalline, medium to coarse grained and subpoilikitic in texture. In some varieties thin layering is well developed. Euhedral to subhedral plagioclase and subhedral to anhedral augite with minor olivine and hornblende are arranged in subpoikilitic manner (Fig. 3c). Plagioclase shows polysynthetic twinning according to albite law. It is mostly labradorite ($An_{52-55}$) and is moderately sericitized. Pyroxene is usually clinopyroxene which is varyingly uralitized. Hypersthene is faintly coloured and pleochroic from pale green to pale reddish brown. It is often anhedral and rounded, and is outwardly altered to hornblende. Pyroxene and olivine may form tiny crystals enclosed in plagioclase. The Model composition of gabbroic rcoks includesplagioclase (pl) 45 – 70%, clinopyroxene (cpx) 15 – 30%, orthopyroxene (opx) 10 – 20%, magnetite and ilmenite. Secondary minerals include hornblende, tremolite, chlorite and sericite. Olivine gabbros contain upto 8% olivine (ol), and their plagioclase is more calcic ($An_{70-72}$). Quartz gabbros contain upto 5% quartz. Hornblende-rich gabbro is melanocratic, holocrystalline, medium to coarse grained and subporphyritic in texture (Fig. 3d).It comprises; plagioclase 50 – 55%, hornblende (hbl), 30 – 40%, augite (Aug), 3 – 5%, olivine, 1 – 3%, magnetite, 1 – 2% and apatite in trace amount.

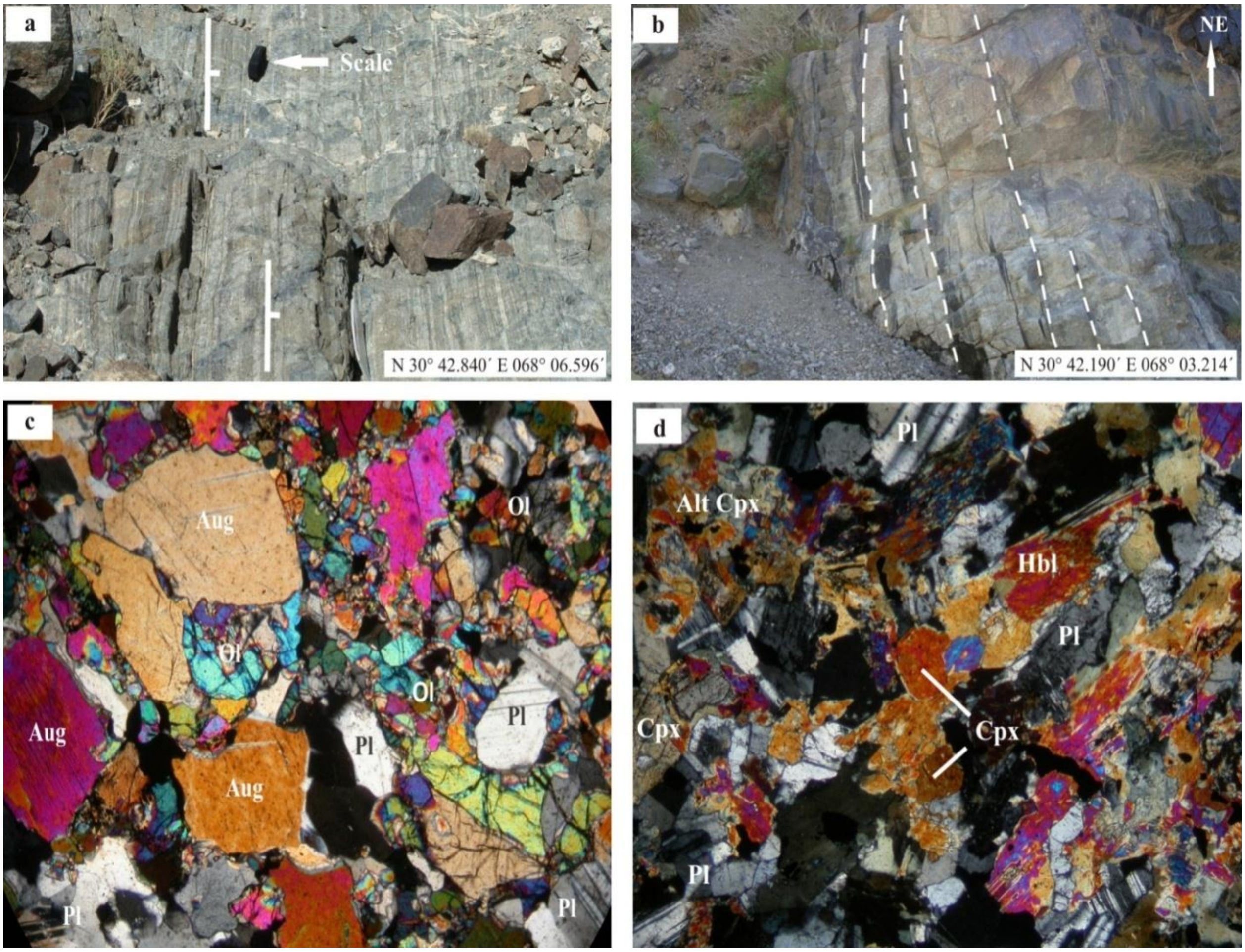


Fig. 3. a) Layered gabbro is trending from base to top and dip to the right; b) Thick gradational layering in gabbro, south of sheeted dyke complex; c) Photomicrograph of gabbro showing subhedral to anhedral plagioclase (pl), augite (aug) with minor olivine (ol) arranged in subpoikilitic manner, XPL x 5; d) photomicrograph of hornblende gabbro showing plagioclase, hornblende (hbl) and altered clinopyroxene (alt cpx) and minor opaque in subporphyritic manner XPL x 5. Mineral symbols from Kretz (1983).

*3.2. Geochemistry*

*3.2.1. Analytical method*

Eleven samples of gabbros were analysed for major and trace elements and three for rare earth elements (REE). The samples were crushed in a jaw crusher. The weathered surfaces were removed and the fresh parts were powdered using a tungsten carbide mill to the size of < 200 mesh. Then the required number of grams of the powder of each sample was heated in a porcelain crucible to $900^0$C for 2 hours to determine the loss on ignition (LOI).

For major elements, the sample powder was thoroughly mixed with lithium tetra-borate (flux) with a 1:5 sample flux ratio and the glass beads were formed. Then the fused beads were analysed for major elements composition using a Philips Wave Dispersive X-Ray Fluorescence (WD/XRF) at the Geoscience Research Laboratories, Geological Survey of Pakistan, Islamabad, Pakistan. For trace elements the powdered pellets of all the samples were prepared by putting 5–7 grams powdered sample (< 200 mesh) in an aluminium cup and compressed between two tungsten carbide plates (within circular briquettes) at about 20 ton per square inch pressure in a hydraulic press. Then these pellets were analysed for trace elements composition using a Philips WD/XRF at the National Centre of Excellence in Geology, University of Peshawar, Pakistan. For REE study the powder was dissolved in 30 ml of 10% $HNO_3$ and 20 ml of de-ionised water. Samples for REE analysis were prepared by a standard Teflon vial acid-digestion procedure using a mixture of HF ± $HClO_4$–$HNO_3$. All samples were spiked to 50 mg / ml with indium to serve as an internal standard. REE analyses for this study were calibrated against a set of multi-element working standard solutions. All the solutions were introduced via a peristaltic pump, and analyses were performed by using a Perkin-Elmer ELAN 6100 Inductively Coupled Plasma Mass Spectrometer (ICP-MS) at the Amdel Laboratories, Pvt. Limited, Adelaide, Australia.

*3.2.2. Classification*

The geochemical data of gabbros obtained through this study are plotted with 03-gabbros published earlier in Khan et al. (2007). The concentration of major, trace and REE of all the gabbros samples are reported in Table 1.

The Muslim Bagh ophiolite gabbros are classified by plotting on total alkali versus $SiO_2$diagram (Cox et al., 1979). All the samples plot in the gabbro field confirming their gabbroic character (Fig. 4). Most of the gabbro samples have very low values of total alkali and $SiO_2$ may be due to their cumulate nature or it could be due to alteration.

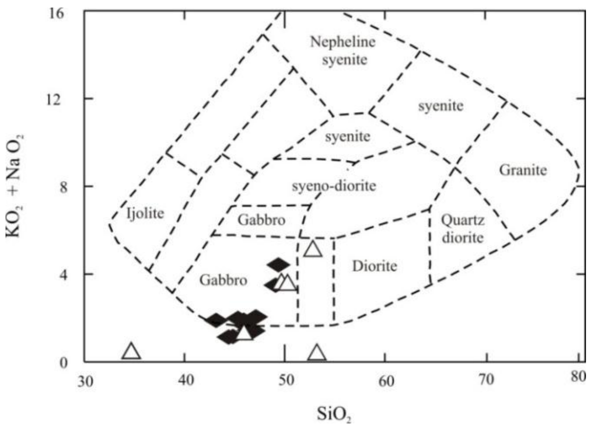


Fig. 4. Total alkali versus $SiO_2$ diagram of the gabbroic rocks from the Muslim Bagh ophiolite (after Cox et al., 1979). Key: Filled diamonds are the gabbros from this study and the triangles are 03-gabbros published earlier in Khan et al. (2007).

*3.2.3. Major elements characteristics*

The Muslim Bagh gabbros have low concentrations (wt. %) of $SiO_2$ (43.16 – 49.58), $TiO_2$ (0.08 –1.13), $Na_2O + K_2O$ (0.6 – 4.42), $P_2O_5$ (0.01– 0.14) and wide ranges of $Al_2O_3$ (14.6 – 29.64), $Fe_2O_3^t$ (2.78 –12.17), MgO (3.25–14.77) and CaO (11.65–17.35). The high concentration of CaO and low concentration of $SiO_2$are due to alteration and the presence of small veinlets of calcite and epidote. The very low $Na_2O + K_2O$ contents can be explained by the cumulate nature of the rocks. This cumulate nature becomes more evident when the $SiO_2$ and MgO are plotted against selected major elements as fractionation index (Fig. 5). In most of the plots the samples cluster together with only minor degree of scattering. The clustering of most of the samples in these plots can be interpreted that these gabbros are less affected by the fractionation and where they scattered, they show their cumulate nature.

Table 1

Major elements (wt %), trace and REE elements (ppm) composition of the gabbros from the Muslim Bagh ophiolite.

| **Rock Name** | **Gab** | **Gab** | **Gab** | **Gab** | **Gab** | **Gab** | **Gab** | **Gab** | **Gab** | **Gab** | **Gab** | **03-Gab** | **03-Gab** | **03-Gab** | **03-Gab** | **03-Gab** | **03-Gab** |
|---|---|---|---|---|---|---|---|---|---|---|---|---|---|---|---|---|---|
| **Sample No** | **C-34** | **C-47** | **C-47A** | **C-48** | **C-49** | **C-50** | **C-51** | **C-54** | **I-91** | **I-147** | **I-175** | **03–5** | **03–6** | **03–8** | **03–11** | **03–13** | **03–16** |
| **$SiO_2$** | 49.38 | 43.16 | 49.58 | 47.12 | 46.21 | 45.34 | 45.91 | 46.12 | 44.42 | 46.43 | 44.85 | 45.89 | 49.63 | 53.35 | 50.24 | 34.64 | 52.77 |
| **$TiO_2$** | 1.13 | 0.08 | 0.64 | 0.54 | 0.28 | 0.72 | 0.62 | 0.12 | 0.12 | 0.35 | 0.25 | 0.24 | 1.06 | 0.12 | 1.69 | 0.62 | 1.12 |
| **$Al_2O_3$** | 15.47 | 29.64 | 15.89 | 18.160 | 18.05 | 17.58 | 18.11 | 14.6 | 22.58 | 18.17 | 16.83 | 16.61 | 14.92 | 2.14 | 14.58 | 11.97 | 14.54 |
| **$Fe_2O_3$** | 10.54 | 2.78 | 8.82 | 11.27 | 8.59 | 12.17 | 10.35 | 5.03 | 5.44 | 11.25 | 8.17 | 7 | 10.04 | 5.72 | 13.07 | 7.81 | 10.96 |
| **MnO** | 0.22 | 0.06 | 0.19 | 0.34 | 0.18 | 0.27 | 0.22 | 0.11 | 0.12 | 0.25 | 0.17 | 0.14 | 0.16 | 0.11 | 0.2 | 0.12 | 0.17 |
| **MgO** | 5.06 | 3.25 | 8.25 | 8.02 | 9.71 | 7.63 | 8.13 | 14.77 | 8.46 | 8.57 | 10.93 | 10.82 | 7.6 | 15.87 | 4 | 4.54 | 4.54 |
| **CaO** | 11.65 | 17.73 | 11.71 | 12.77 | 15.67 | 14.05 | 14.95 | 16.91 | 17.35 | 13.5 | 16.94 | 18.59 | 9.11 | 19.13 | 8.63 | 22.75 | 6.92 |
| **$Na_2O$** | 3.94 | 1.24 | 2.81 | 1.49 | 0.8 | 1.41 | 1.34 | 0.56 | 0.58 | 0.88 | 0.61 | 0.66 | 3.01 | 0.09 | 3.16 | 0.35 | 4.44 |
| **$K_2O$** | 0.48 | 0.12 | 0.67 | 0.03 | 0.04 | 0.04 | 0.03 | 0.56 | 0.02 | 0.03 | 0.02 | 0.05 | 0.52 | 0.04 | 0.33 | 0.03 | 0.6 |
| **$P_2O_5$** | 0.14 | 0.01 | 0.14 | 0.09 | 0.01 | 0.07 | 0.04 | 0.03 | | 0.01 | | 0.18 | 0.28 | 0.13 | 0.1 | 0.25 | 0.44 |
| **LOI** | 1.99 | 1.94 | 1.29 | 0.171 | 0.45 | 0.72 | 0.3 | 1.74 | 0.91 | 0.57 | 1.23 | 1.1 | 3.29 | 2.27 | 2.08 | 19.29 | 2.98 |
| **Total** | **100** | **100.01** | **99.99** | **100.001** | **99.99** | **100** | **100** | **100.55** | **100** | **100.01** | **100** | **101.28** | **99.62** | **98.97** | **98.08** | **102.37** | **99.48** |
| **Sc** | 329.3 | 17.6 | 35.7 | 39.6 | 43.4 | 45.2 | 47.2 | 40.2 | 39.7 | 46.5 | 52.4 | 65.5 | 35.6 | 106.8 | 33.8 | 24.5 | 31.1 |
| **V** | 28.9 | 42.2 | 245.5 | 159.3 | 171.4 | 325.6 | 258.4 | 89.4 | 110.9 | 263.8 | 172.3 | 203 | 245 | 172 | 389 | 154 | 234 |
| **Cr** | 28.9 | 21.4 | 193.9 | 14.3 | 105.2 | 29.7 | 34.9 | 888.8 | 84.5 | 53.8 | 61.3 | 59 | 59 | 1224 | 24 | 585 | 61 |
| **Co** | 50 | 29.3 | 52.8 | 66.3 | 70 | 72.7 | 66.7 | 59.9 | 66.2 | 66.8 | 67.7 | 35 | 35 | 50 | 36 | 36 | 30 |
| **Ni** | 25 | 22.7 | 52 | 14.2 | 39.7 | 27.5 | 32.7 | 194.1 | 46 | 42.9 | 49.4 | 57 | 50 | 608 | 26 | 215 | 36 |
| **Zn** | 85 | 5.6 | 52.6 | 100 | 32.7 | 67.4 | 49.9 | 14.9 | 19.5 | 74.7 | 21.1 | 5 | 40 | 0 | 67 | 27 | 99 |
| **Ga** | 17.5 | 25.6 | 26.6 | 28.1 | 25.3 | 28.6 | 26.9 | 19.4 | 13.5 | 28 | 23.8 | 10.5 | 15.7 | 2.2 | 16.8 | 22.3 | 16.3 |
| **Sr** | 251.3 | 394.7 | 231.9 | 297 | 237.9 | 286 | 249.3 | 94 | 269.5 | 85.5 | 196 | 222 | 289 | 11 | 192 | 32 | 63 |
| **Y** | 22.3 | 1.9 | 14.7 | 7.8 | 6.3 | 9.5 | 12.7 | 3.3 | 2.4 | 6.4 | 4.9 | 5.3 | 24.9 | 1.8 | 24 | 15.8 | 31.5 |
| **Zr** | 71.7 | 20 | 62 | 15.1 | 13.1 | 15.1 | 19.8 | 5.5 | 12.1 | 5.7 | 10.8 | 19 | 64 | 7 | 64 | 29 | 85 |
| **Nb** | 0.5 | | 2.3 | 0.4 | | 0.3 | 1.1 | 0.2 | 0.2 | 0.3 | 0.2 | 0.89 | 0.11 | 0.12 | 1.99 | 1.23 | 3.11 |
| **Ba** | 227.5 | 60.4 | 129.1 | 44.7 | 33.5 | 54 | 48 | 12.6 | 7.3 | 14.1 | 20.8 | 14.2 | 113.8 | 10.4 | 97.8 | 11.3 | 84.4 |
| **La** | 3.5 | 8.9 | 9 | 4.2 | 4 | 7.3 | 11.1 | 0.8 | 2.5 | 3.1 | 11.9 | 2.22 | 0.17 | 0.2 | 3.24 | 2 | 5.7 |
| **Ce** | 7.1 | 8.1 | 8.6 | 8.4 | 7.7 | 10.9 | 20.8 | 15.9 | 5.3 | 8.2 | 0.5 | 6.75 | 0.78 | 0.59 | 9.81 | 5.78 | 16.95 |
| **Nd** | 8.5 | 0.1 | 11.5 | 3 | 7.3 | | 1.7 | 36.8 | 0.72 | 4.9 | 7.8 | 5.5 | 1.24 | 0.51 | 7.69 | 4.46 | 12.86 |
| **Sm** | 3.3 | | | 0.96 | 2.8 | | | 9.6 | 0.22 | | | 1.85 | 0.56 | 0.2 | 2.48 | 1.42 | 3.72 |
| **Yb** | 2.7 | | | 0.8 | | | | 14.1 | 0.2 | | | 2.13 | 0.55 | 0.16 | 2.54 | 1.59 | 3.17 |
| **Hf** | 23.6 | 18.4 | 20.1 | 22.6 | 20.5 | 16.1 | 25.6 | 22.7 | 28.1 | 24.7 | 23.5 | 0.13 | 1.75 | 0.2 | 1.68 | 1.03 | 2.08 |
| **Ta** | 6.2 | | 4.9 | 3.6 | 2.7 | 5.3 | 8.9 | 3.8 | 2.2 | 2.3 | 3.5 | | 0.15 | 0 | 0.15 | 0.15 | 0.18 |
| **Th** | 2.4 | 1.9 | 0.44 | 2.1 | 3.6 | 1.3 | 1.71 | 0.9 | 6.5 | 0.8 | 0.94 | 0.33 | 0.01 | 0.02 | 0.35 | 0.2 | 0.49 |
| **Tm** | 0.4 | | | 0.1 | | | | | | | | 0.32 | 0.09 | 0.03 | 0.37 | 0.23 | 0.49 |
| **Tb** | 0.64 | | | 0.2 | | | | | 0.06 | | | 0.46 | 0.15 | 0.05 | 0.59 | 0.36 | 0.75 |
| **Pr** | 1.7 | | | 0.6 | | | | | 0.2 | | | 1.11 | 0.18 | 0.1 | 1.59 | 0.92 | 2.78 |
| **Lu** | 0.16 | | | | | | | | | | | 0.32 | 0.08 | 0.03 | 0.37 | 0.23 | 0.46 |
| **Ho** | 0.88 | | | 0.28 | | | | | 0.08 | | | 0.65 | 0.2 | 0.07 | 0.78 | 0.49 | 1.01 |
| **Gd** | 3.3 | | | 1.1 | | | | | 0.25 | | | 2.43 | 0.78 | 0.27 | 3.26 | 1.95 | 4.34 |
| **Eu** | 1.15 | | | 0.7 | | | | | 0.16 | | | 0.73 | 0.26 | 0.08 | 1.07 | 0.52 | 1.03 |
| **Er** | 2.7 | | | 0.85 | | | | | 0.2 | | | 1.96 | 0.58 | 0.19 | 2.41 | 1.52 | 3.06 |
| **Dy** | 4.5 | | | 1.45 | | | | | 0.4 | | | 3.23 | 1.03 | 0.35 | 4.05 | 2.47 | 5.11 |

**Note:** LOI = Loss On Ignition at 1000$^{o}$C, $Fe_2O_3$ = total iron, Gab = Gabbro, 03-Gab = 03-Gabbros, which are from Khan et al., 2007

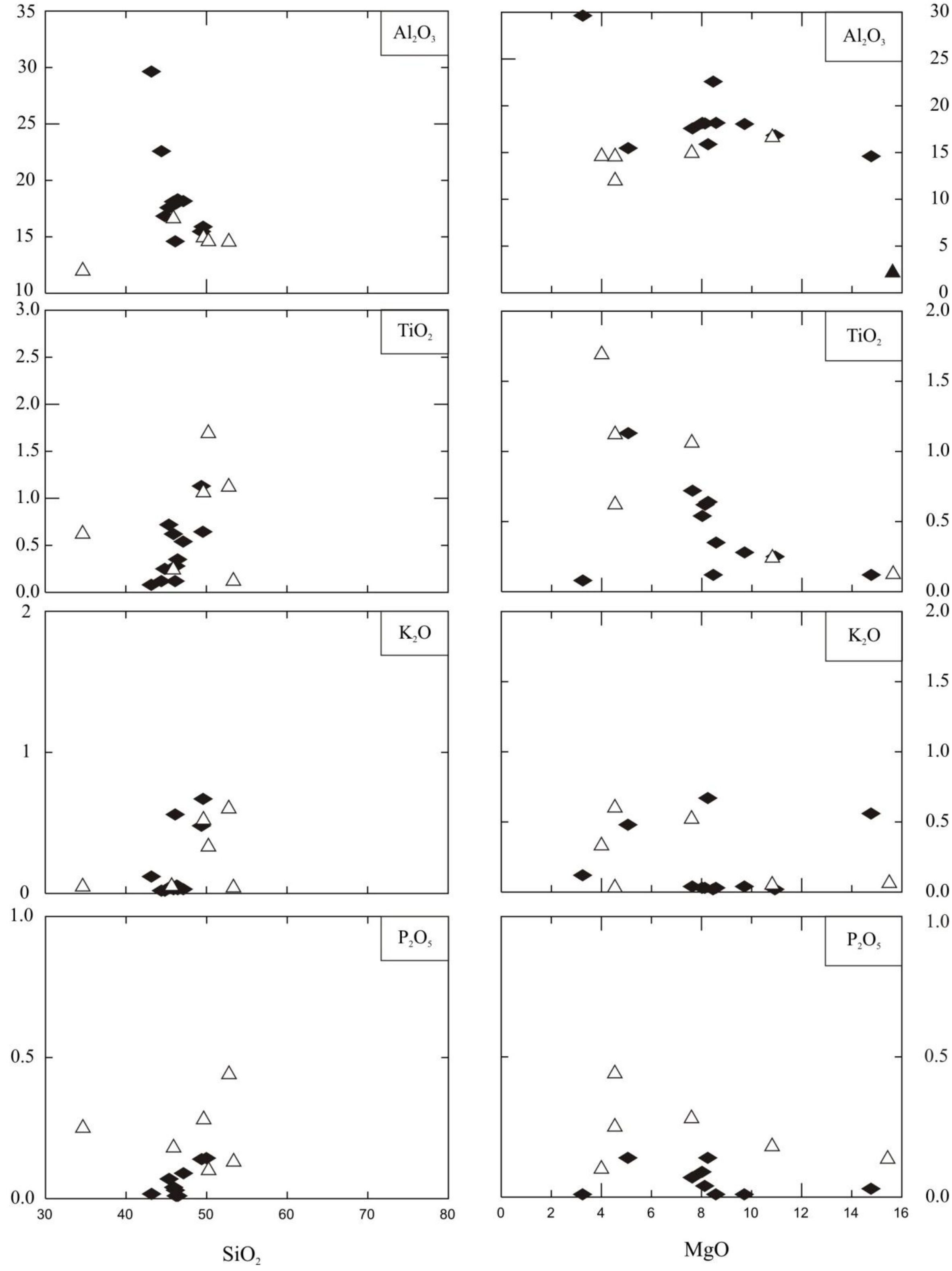
Al2O3
TiO2
K2O
P2O5
SiO2
MgO

Fig. 5. $SiO_2$ and MgO versus selected major elements plots of the Muslim Bagh gabbros. The symbols are the same as in Figure 4.

### *3.2.4. Trace and rare earth elements (REE) characteristics*

The Muslim Bagh gabbros have variable concentrations of both Large-ion lithophile (LIL) elements (in ppm) such as Ba (7.3–227.5), Rb (1–10.2), K (200–6700), Sr (85.5–394.7), Ce (10.9–55.9), and HFS-elements like Zr (5.5–71.7), Y (3.3–22.3) and Nb (0.2–5.5). These rocks are variably altered and metamorphosed to greenschist facies. The alteration is obvious from the wider range of CaO (11.65–17.35) and LOI content (0.3–1.99). So it is expected that the large-ion lithophile (LIL) elements (Rb, K, Ba, Sr) have been remobilized to variable degree during these alteration processes (Humphris and Thompson, 1978; Staudigel, 2003).

Zr is plotted against the high field strength (HFS) elements (Nb, Y, Ti, P) in Figure 6. These plots show a linear relationship with some degree of scatter probably in rocks having cumulate phases. These trends show that all the gabbroic rocks are probably formed from a single parental magma through the process of fractional crystallization. It further confirms that the HFS-elements are less-affected by secondary alteration, so the data for these elements will be reliable to use for the petrogenesis and tectonic setting of these rocks.

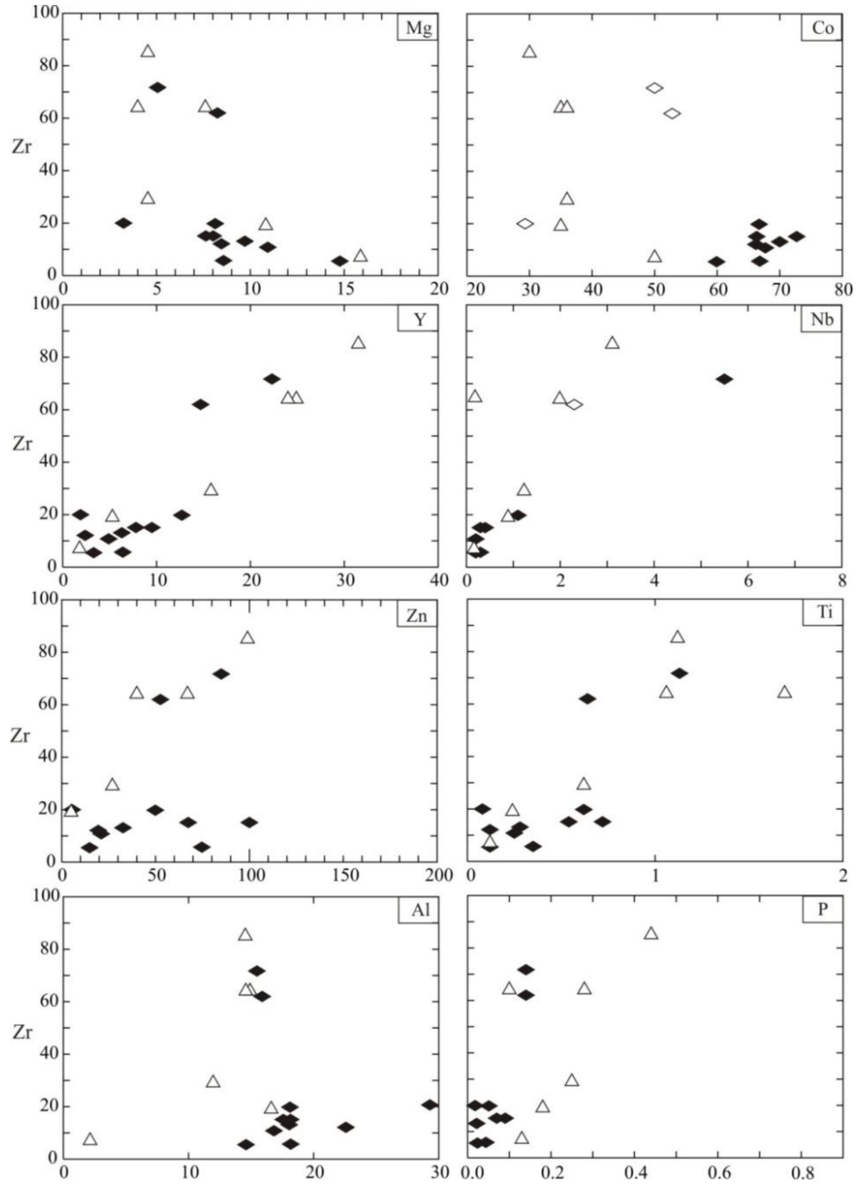

Fig. 6. Zr versus major and trace elements plots of the Muslim Bagh gabbros. For symbols see Figure 4.

The trace and REEs of the Muslim Bagh gabbros are evaluated by plotting on multi-element normalised diagrams (Fig.7a-b). In the N-MORB normalized pattern (Sun and McDonough, 1989) of these gabbros the HFS-elements (P, Zr, Sm, Ti, and Y) show a flat pattern parallel to MORB. In contrast, the LIL-elements (Rb, Ba, Th, Sr) are relatively more enriched than MORB. While REE patternis almost flat having slightly positive Eu anomalies. The enrichment in LIL-elements may be due to the addition of a subduction component to N-MORB source (e.g., Wood, 1980; Pearce et al., 1984; Saunders and Tarney, 1991). The positive Eu anomaly reflects accumulation of plagioclase.

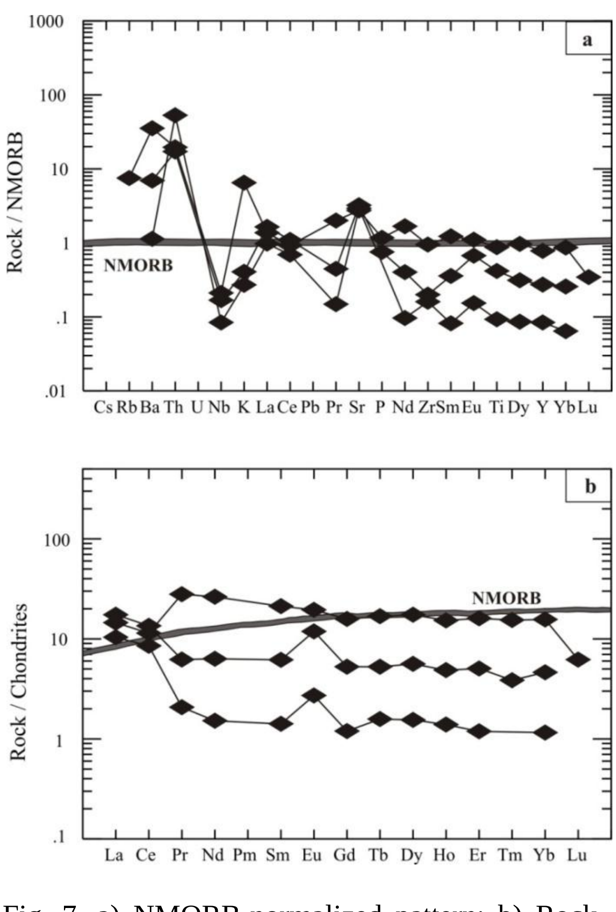


Fig. 7. a) NMORB-normalized pattern; b) Rock /Chondrite REE pattern (after Sun and McDonugh, 1989).

## 4. Discussion

The Muslim Bagh ophiolite gabbros include olivine gabbro, gabbro-norite, norite and hornblende gabbro. They show the characteristics of tholeiitic igneous rocks as evidenced by the low ratio of Zr/Ti (0.0016–0.025) and Nb/Y (0.0044–0.2466) and their plot as basaltic rocks on Zr/Ti–Nb/Y diagram (Fig. 8a) of Pearce, (1996), and as tholeiite on $TiO_2$ versus Zr/ ($P_2O_5$*$10^4$) (Fig. 8b) of Winchester and Floyd (1976). The geochemical features of the major and trace elements show that the rocks have both cumulates and non-cumulates phases and that all the three minerals; olivine, pyroxenes and plagioclases (ol + pyx + pl) are involved in the fractionation process. This type of mineralization is typical of decompression setting over a subduction zone (Pearce et al., 1984).

Several attributes of the gabbroic rocks of the Muslim Bagh ophiolite point to the tectonic setting of magma generation responsible for their formation. The tectonic discrimination diagrams e.g. Nb/Th versus Y (Fig. 8c) of Jenner et al., (1991), plot these gabbros in the arc field, and Ti/100 – Zr – Y*3 diagram (Fig. 8d) of Pearce and Cann (1973), classify the gabbros as both island arc tholeiite (IAT) and depleted mantle oceanic floor basalt (N-MORB). From Pearce and Cann (1973), diagram none of the samples from gabbros is found to plot in the field of either within plate basalt (WPB), enriched mid oceanic ridge Basalt (E-MORB) or the calc-alkaline basalt (CAB) field. There is a possibility that these gabbros may have a transitional character between the IAT and N-MORB and so it is likely that these gabbros have formed by fractionation in a low pressure extensional environment directly over a subduction zone or in the supra-subduction zone. The transitional character of the gabbros from the Muslim Bagh ophiolite between IAT and N-MORB is also indicated by their normalized trace and REE diagrams (Fig. 7a-b). In the NMORB-normalized plot the HFS-elements (P, Zr, Sm, Ti, and Y) and in the rocks/Chondrites plot of the REE show more or less flat pattern depicting NMORB affinity. While the enrichment of the LIL-elements (Rb, Ba, Th, Sr) with no depletion in the LREE, along with depletion in Nb, suggests addition of a subduction component to the depleted mantle source. The supra-subduction setting of the gabbroic rocks from the Muslim Bagh ophiolite is further confirmed when major element compositions are plotted on the AFM diagram of Beard (1986). Most of the gabbro samples plot in the arc-related mafic cumulate field, whereas some samples plot in the arc-related non-cumulate field (Fig. 9). This implies that both the cumulate and non-cumulate gabbroic rocks formed in a supra-subduction zone tectonic setting.

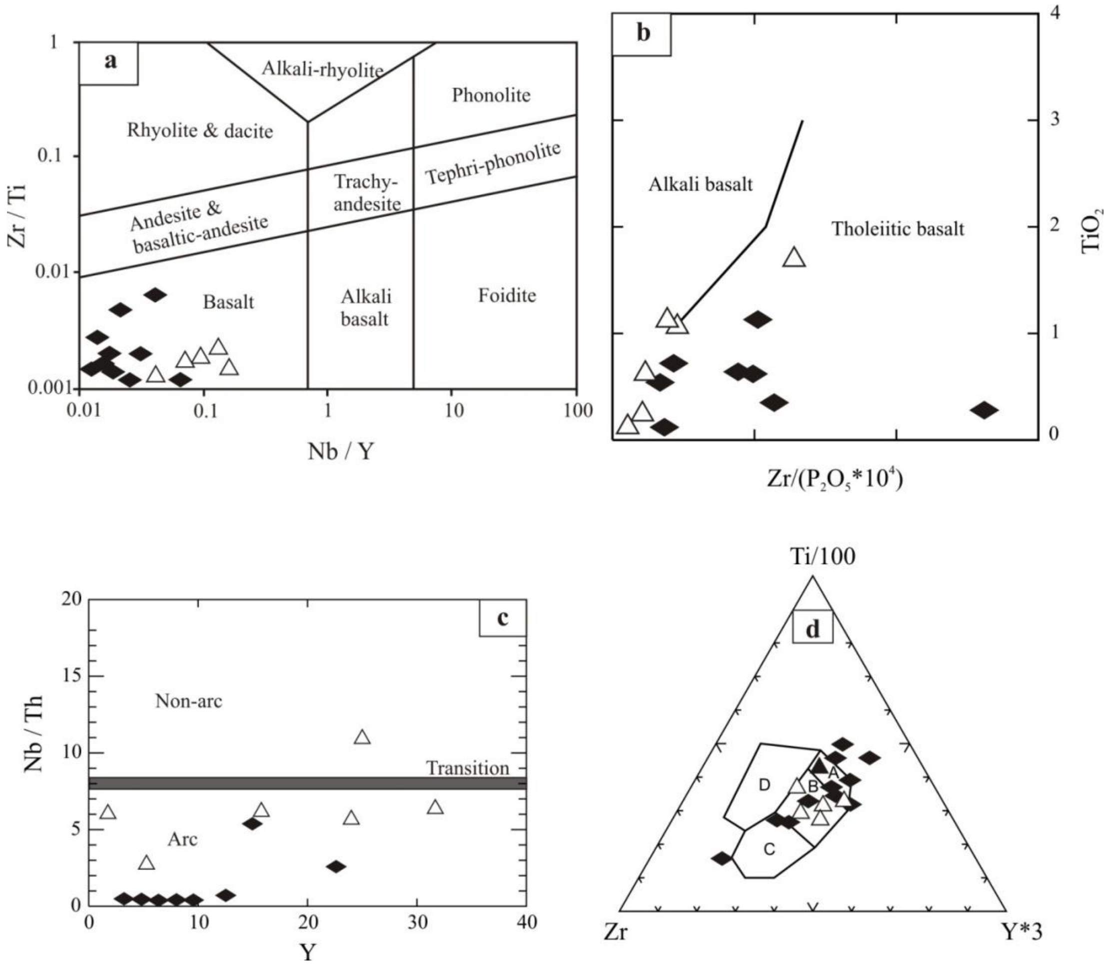


Fig. 8. a) Zr/Ti–Nb/Y plot (after Pearce, 1996); b) TiO2 versus Zr/ (P2O5* 104) (after Winchester and Floyd, 1976); c) Nb/Th–Y plot (after Jenner et al., 1991); d) Ti/100 – Zr – Y*3 triangular plot (after Pearce and Cann (1973). Key for Fig. d; A = Island arc, B = Ocean floor, C = Calc alkali and D = Within plate.

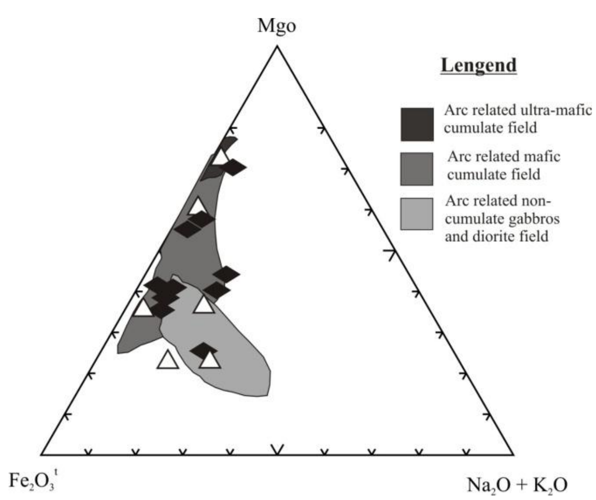


Fig. 9. AFM diagram after Beard (1986). See text for description. Symbols are the same as in Figure 4.

## 5. Conclusions

The crustal part of the Muslim Bagh ophiolite has a less developed gabbroic section with relatively thick ultramafic-mafic cumulates section. The gabbros are olivine gabbro, norite, gabbro-norite and hornblende gabbro. They are identified both cumulates and non-cumulates with olivine, clinopyroxine, orthopyroxene and plagioclase as their principle minerals that are all involved in the fractionation processes. The enrichments of LIL-elements and depletion of Nb, transitional characteristics between the NMORB and IAT, suggest supra-subduction zone tectonic setting for Muslim Bagh gabbros.


## Acknowledgments

Geochemical analyses are financed by the Higher Education Commission, Pakistan through their Access to Scientific Instrumentation, and International Research Support Initiative Program funds to M. Ishaq Kakar. The reviewers are greatly acknowledged for their constructive comments.


## References


Ahmed, Z., Abbas, S.G., 1979. The Muslim Bagh Ophiolites. In: Farah, A., DeJong, K.A. (Eds.), Geodynamics of Pakistan. Geological Survey of Pakistan, Quetta, 243-250.

Asrarullah, Ahmad, Z., Abbas, S.G., 1979. Ophiolites in Pakistan: An introduction. In: Farah, A., DeJong, K.A. (Eds.), Geodynamics of Pakistan. Geological Survey of Pakistan, Quetta, 181-192.

Beard, J.S., 1986. Characteristic mineralogy of arc related cumulate gabbros: implications for the tectonic setting of gabbroic plutons and for andesite genesis. Geology, 14, 848-851.

Bedard, J. H., 1991. Cumulate recycling and crustal evolution in the Bay of Islands ophiolite. Journal of Geology, 99, 225-249.

Bilgrami, S.A., 1964. Mineralogy and petrology of the central part of the Hindu Bagh Igneous complex, Hindu bagh Mining District, Zhob Valley. West Pakistan Geological Survey Records, 10, 28.

Cox, K.G., Bell, J.D., Pankhurst, R.J., 1979. The Interpretation of Igneous Rocks. Allen and Unwin, London.

Humphris, S.E., Thompson, G., 1978. Trace element mobility during hydrothermal alteration of oceanic basalts. Geochimica et Cosmochimica Acta, 42, 127-136.

Jenner, G.A., Dunning, G.R., Malpas, J., Brown, M., Brace, T., 1991. Bay of Islands and Little Port complexes, revisited: age, geochemical and isotopic evidence confirm supra-subduction zone origin. Canadian Journal of Earth Sciences, 28, 135-162.

Khan, M., Kerr, A.C., Mahmood, K., 2007. Formation and tectonic evolution of the Cretaceous–Jurassic Muslim Bagh ophiolitic complex, Pakistan: Implications for the composite tectonic setting of ophiolites. Journal of Asian Earth Sciences, 31, 112-127.

Kretz, A., 1983. Symbols for rock forming minerals. American Mineralogist, 68, 277-279.

Mahmood, K., Boudier, F., Gnos, E., Monié, P., Nicolas, A. 1995. $^{40}Ar$ / $^{39}Ar$ dating of the emplacement of the Muslim Bagh ophiolite, Pakistan. Tectonophysics, 250, 169-181.

Mahmood, K., Khan. M. 1999. Structural characteristics of Gabbroic rocks from Saplai Tor Ghar Massif, Muslim Bagh ophiolite, Pakistan. Acta Mineralogica Pakistanica, 10, 27-36.

Nicolas, A., 1989. Structures of Ophiolites and Dynamics of Oceanic Lithosphere. Kluwer, Dordrecht.

Pearce, J.A., 1996. A user's guide to basalt discrimination diagrams. In: Bailes, A. H., Christiansen, E.H., Galley, A.G., Jenner, G.A., Keith, Jeffrey, D., Kerrich, R., Lentz, David, R., Lesher, C.M., Lucas, Stephen B., Ludden, J.N., Pearce, J.A., Peloquin, S.A., Stern, R.A., Stone, W.E., Syme, E.C., Swinden, H.S., Wyman, D.A., (Eds.), Trace element geochemistry of volcanic rocks; applications for massive sulphide exploration, Short Course Notes-Geological Association of Canada, 12, 79-113.

Pearce, J.A., Cann, J.R., 1973. Tectonic setting of basic volcanic rocks determined using trace element analysis. Earth and Planetary Science Letters, 19, 290-300.

Pearce, J.A., Lippard, S.J., Roberts, S., 1984. Characteristics and Tectonic significance of supra-subduction ophiolites. In: Kokelaar, B.P., Howels, M.F. (Eds.), Marginal Basin Geology. Geological Society London Special Publications, 16, 77-94.

Penrose Conference, 1972. Penrose field conference on ophiolites, Geotimes, 17, 24-25.

Saunders, A.D., Tarney, J., 1991. Back-arc basins. In: Floyd, P. (Ed.), Ocean Basalts. Blackie, London, 219-263.

Siddiqui, R.H., Aziz, A., Mengal, J.M., Hoshino, K., Sawada, Y., 1996. Geology, Petrochemistry and Tectonic Evolution of Muslim Bagh Ophiolite Complex Balochistan, Pakistan. Geologica; Geoscience Laboratories, Geological Survey of Pakistan, 3, 11-46.

Staudigel, H., 2003. Hydrothermal alteration processes in the oceanic crust. In: Holland, H.D., Turekian, K.K., (Eds.), Treatise on geochemistry, 3, 511-535.

Sun, S.-S., McDonough, W.F., 1989. Chemical and isotopic systematics of oceanic basalts: Implications for mantle com In: Saunders, A.D., Norry, M.J. (Eds.), Magmatism in the Ocean Basins. Geological Society Special Publication, 42, 313-345.

Van Vloten, R., 1967, Geology and chromite deposits of the Nisai area, Hindu Bagh mining district, West Pakistan. Geological Survey of Pakistan, 2, 32.

Winchester, J.A., Floyd P.A., 1976. Geochemical magma type discrimination: Application to altered and metamorphosed igneous rocks. Earth and Planetary Science Letters, 28, 459-469.

Wood, D.A., 1980. The application of a Th-Hf-Ta diagram to problems of tectono-magmatic classification and to establishing the nature of crustal contamination of basaltic lavas of the British Tertiary volcanic province. Earth and Planetary Science Letters, 50 (1), 11-30.